

Intermittent dipping in a low-mass X-ray Binary

Duncan K. Galloway,^{1,2*} Alishan N. Ajamyan,¹ James Upjohn¹
and Matthew Stuart³

¹*School of Physics & Astronomy, Monash University, VIC 3800, Australia*

²*also Monash Centre for Astrophysics, Monash University, VIC 3800, Australia*

³*School of Mathematical Sciences, Monash University, VIC 3800, Australia*

Accepted 2016 June 29. Received 2016 June 29; in original form 2016 May 30

ABSTRACT

Periodic dips observed in $\approx 20\%$ of low-mass X-ray binaries are thought to arise from obscuration of the neutron star by the outer edge of the accretion disk. We report the detection with the *Rossi X-ray Timing Explorer* of two dipping episodes in Aql X-1, not previously a known dipper. The X-ray spectrum during the dips exhibited an elevated neutral column density, by a factor between 1 and almost two orders of magnitude. Dips were not observed in every cycle of the 18.95-hr orbit, so that the estimated frequency for these events is $0.10^{+0.07}_{-0.05} \text{ cycle}^{-1}$. This is the first confirmed example of intermittent dipping in such a system. Assuming that the dips in Aql X-1 occur because the system inclination is intermediate between the non-dipping and dipping sources, implies a range of $72\text{--}79^\circ$ for the source. This result lends support for the presence of a massive ($> 2 M_\odot$) neutron star in Aql X-1, and further implies that ≈ 30 additional LMXBs may have inclinations within this range, raising the possibility of intermittent dips in those systems also. Thus, we searched for dips from 24 other bursting systems, without success. For the system with the largest number of dip phases covered, 4U 1820–303, the nondetection implies a 95% upper limit to the dip frequency of $1.4 \times 10^{-3} \text{ cycle}^{-1}$.

Key words: X-rays: binaries – accretion discs – X-rays: individual: Aql X-1

1 INTRODUCTION

Periodic, irregular dips in the X-ray intensity of low-mass X-ray binaries (LMXBs) were first observed in the early 1980s (White & Mason 1985). The dips are generally attributed to partial obscuration of the neutron star by a thickened region of the accretion disk close to the line joining the two centres of mass (e.g. Díaz Trigo et al. 2006). The dips are typically irregular in shape and depth, with duty cycle between 10–30%, and (in most systems) are accompanied by an increase in the absorption column density.

XB 1916–050 was the first such example discovered (White & Swank 1982; Walter et al. 1982), with dips recurring at the ≈ 50 min orbital period. White & Mason (1985) described 4 systems showing periodic dips, and one additional system (X 1624–490) in which the dips were not yet known to be periodic. Since then, the list of known dippers has grown to include EXO 0748–676, 4U 1254–69 (XB 1254–690), MXB 1659–298, 4U 1746–371, 4U 1323–62, XTE J1710–281, GRS 1747–312, and possibly also XTE J1759–220 and 1A 1744–361, (e.g. Liu et al. 2007). The most recent discovery of dipping behaviour is in the 24.27-d binary and burst source, GX 13+1 (Iaria et al. 2014).

The dips are characterised by a decrease in X-ray intensity, and (usually) an increase in spectral hardness, arising from addi-

tional absorption at the low-energy (< 10 keV) part of the X-ray spectrum. The lack of photoabsorption in shallow dips seen from X 1755–338 was explained by metal-poor obscuring material; the required abundances are 1/600 of the solar value. Similarly, a factor 10–60 shortfall in degree of photoelectric absorption was also noted for XB 1916–50 (White & Mason 1985).

Dips may occur over $\approx 30\%$ of the orbital cycle, generally just prior to inferior conjunction, and culminating in some sources (EXO 0748–676 and MXB 1659–298) in an eclipse (e.g. Parmar et al. 1986; Cominsky & Wood 1984). The inclination angle for dipping sources is thought to be higher than for the non-dippers, and for the systems which also show eclipses is higher again (e.g. Motch et al. 1987).

Conventionally, the sample of LMXBs was clearly divided into dippers (which showed a dip in almost every orbital cycle) and non-dippers, which never exhibited dips. A possible exception was the candidate absorption event reported from the ultracompact binary 4U 1820–303 (Cominsky et al. 1985) following a search for high hardness ratios with HEAO A-2. Scanning observations of the source were made between 1977 August and 1978 March; one of the scans, on 1977 Sep 27, 23:33:56 UT, was found with hardness ratio increased compared to previous scans by a factor of almost 3. The neutral column density was inferred to have increased for the “abnormal” scan. Because of the low duty cycle of the scanning observations, the duration of the event was not well constrained

* E-mail: duncan.galloway@monash.edu

(≤ 2 hr; Morgan et al. 1988), although the variation was seemingly not related to the (energy-independent) orbital X-ray intensity modulation.

Recently, a single dipping event was observed by the *Rossi X-ray Timing Explorer* (*RXTE*) from the 18.95-hr binary Aql X-1 (Galloway 2012), not previously known as a dipping source. Aql X-1 is one of the most prolific X-ray transients known, exhibiting bright ($L_X \approx 10^{37}$ ergs s $^{-1}$) outbursts every few hundred days since 1969 (e.g. Campana et al. 2013). The transient outburst profiles are quite variable, with a range of durations and fluences noted by several authors (e.g. Güngör et al. 2014). In recent years, the source has exhibited “long high” outbursts in 2011 and 2013, and weaker outbursts in each of the following years (e.g. Waterhouse et al. 2016).

Here we describe in more details the properties of the event observed from Aql X-1, and also report on a search for additional dipping events in a large sample of LMXBs.

2 OBSERVATIONS AND ANALYSIS

We analysed *Rossi X-ray Timing Explorer* (*RXTE*) observations of low-mass X-ray binaries assembled for the Multi-INstrument Burst ARchive (MINBAR¹). *RXTE*, operational from its launch on 1995 December 30 through to the end-of-mission on 2012 January, consists of three instruments sensitive to cosmic X-rays: the All-Sky Monitor (ASM), the High-Energy X-ray Timing Experiment (HEXTE), and the Proportional Counter Array (PCA). The PCA is comprised of five identical Proportional Counter Units (PCUs), sensitive to photons in the 2–60 keV energy range, and together presenting an effective area of approximately 6500 cm² (Jahoda et al. 1996). The field-of-view is approximately circular with a radius of 1 degree, determined by a passive hexagonal-lattice collimator, and the instrument offers no spatial resolution. Photons detected by the PCA are time-tagged to a precision of approximately 1 μ s, and processed by an array of on-board event analysers (EAs). Two of the EAs are dedicated to producing standard-mode analysis results; Standard-1 data offers no spectral resolution but 0.125 s binned lightcurves, while Standard-2 data offers spectra accumulated every 16 s within 129 spectral channels covering the energy range.

The MINBAR project builds on an earlier sample of bursts observed by *RXTE* (Galloway et al. 2008), and seeks to accumulate all observations of burst sources by *RXTE* as well as *BeppoSAX*/WFC and *INTEGRAL*/JEM-X. As part of the data analysis pipeline for the MINBAR observations, we calculated soft and hard X-ray colours from the background-subtracted Standard-2 lightcurves, as the ratio of counts in the 3.7–4.9 keV and 2–3.7 keV bands, and the 8.6–17.7 keV and 4.9–8.6 keV bands, respectively. In contrast to the analysis of Galloway et al. (2008), we made no correction for the gain changes throughout the lifetime of the instrument, as we focused on searches for dipping events usually within a single ≈ 90 min orbit.

The dipping activity in Aql X-1 during the observation on 2011 October 21 (MJD 53715) was discovered serendipitously via inspection of the lightcurve around the time of a thermonuclear burst (Galloway 2012, see also §3). The dips were characterised by both soft and hard colours significantly in excess of the typical measurements before and after, in addition to a decrease in intensity. We subsequently used this event as a template to perform an

exhaustive search in this and other systems with a substantial accumulated exposure with *RXTE*, as follows.

First, we filtered the colour measurements to exclude intervals with high variance, including unphysically large positive or negative values, usually attributable to low source intensity, e.g. at the end of a transient outburst.

Second, we divided the available data from each source into contiguous segments, in which the maximum allowed gap between segments was 0.006 d. We further selected only data segments with at least 10 data points, as it would not be possible to confirm a dip in a sparser segment.

From each segment we calculated the mean \bar{C}_b and standard deviation σ_b for each band b (hard and soft colours), and identified candidate events as high-significance outliers from the average distribution. We estimated the significance as

$$S_{b,i} = \frac{C_{b,i} - \bar{C}_b}{\sigma_b} \quad (1)$$

and inspected only those measurements where $S_{b,i}$ was in excess of a threshold established empirically from the analysis of the Aql X-1 data, of $S_{b,i} > 5$.

Finally, we inspected the intensity data covering the dip candidate, to test for the coincident decrease in intensity expected for a genuine dipping event.

3 RESULTS

The first instance of dipping behaviour detected from Aql X-1 was in an observation by *RXTE* on 2011 October 21 (obsid 96440-01-02-02), eight days after the detection of a new outburst (Yamaoka et al. 2011). Beginning on October 21.579 UT (MJD 55855.583), a series of four dips were observed in the X-ray intensity, lasting between 5–60 s each (Fig. 1). The first two dips were separated by 3.9 min; then 7.8 min to the next two (which occurred as a closely separated pair), and 9 min to the last. The observation ended 3 min later. During the second (and deepest) dip, the count rate was reduced to less than 20% of the level before or after; the other dips reached between 38–67% of the count rate before or after. One proportional counter unit (PCU #2) was operating, and the background-subtracted 2–60 keV count rate outside the dips was typically 470 counts s $^{-1}$.

The fractional decrease in intensity during the dips was greatest at low energies (Fig. 1), resulting in a hardening of the X-ray spectrum. Both the soft and hard X-ray colours were significantly higher compared to the non-dip data. During the second (and deepest) dip, the soft (hard) colour reached 4.0 (1.39), compared to 1.3 (0.8) outside the dips. These values were discrepant from the mean colours for the observation at an estimated significance of 8.3 (6.4) σ (Table 1).

3.1 Search for additional dips from Aql X-1

We carried out a search (as described in §2) for similar events in the entire sample of *RXTE* observations of Aql X-1, totalling 1.85 Ms (Table 3). One additional candidate was found, on 2005 December 11 (MJD 53715.173), almost 6 years before the 2011 October event. This observation fell approximately one month after the start of the most recent outburst, which likely began on 2005 November 12 (Rodríguez & Shaw 2005). Only one interval with substantial ($\approx 40\%$) reduction in intensity was observed in 2005 December,

¹ <http://burst.sci.monash.edu/minbar>

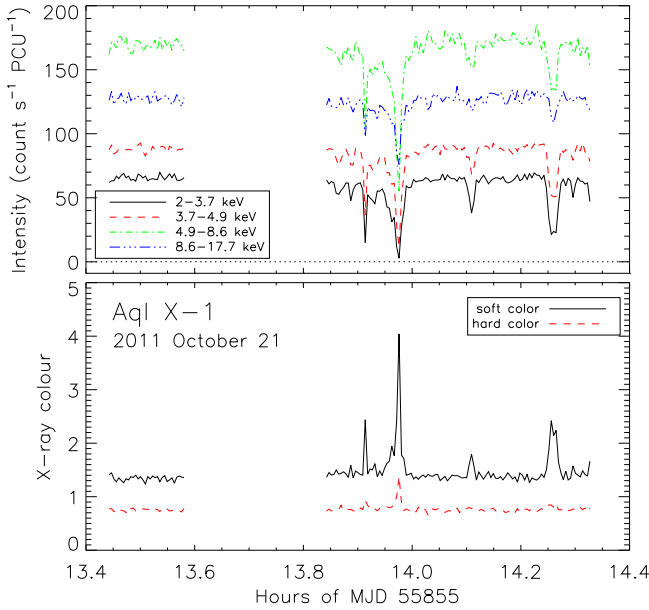


Figure 1. X-ray intensity of Aql X-1 on 2011 October 21 as a function of energy, calculated from 16-s binned Standard-2 mode data. The X-ray intensity in the 2–3.7 keV, 3.7–4.9 keV, 4.9–8.6 keV and 8.6–17.7 keV bands (top panel) shows that the dip is deepest at lower energies, producing an overall harder X-ray spectrum. This hardening of the spectrum is confirmed by the soft and hard X-ray colours (calculated from the ratio of 3.7–4.9 keV to 2–3.7 keV intensity, and 8.6–17.7 keV to 4.9–8.6 keV, respectively; bottom panel).

lasting approximately 34 s. The dip onset was gradual, but the recovery much steeper, similar in profile to the deepest dipping event observed in 2011 October. Four PCUs were active during the observation, but the intensity was lower than for the 2011 October event, by approximately a factor of two. The significance of the maximum deviation from the colour measurements during the observation was similar in both cases, at $6\text{--}8\sigma$ (Table 1).

We also list in Table 1 the orbital phase range of the dip activity, based on the ephemeris for the 18.95-hr orbit adopted by Welsh et al. (2000). We calculated the phase φ_i of each data point at time t_i , via

$$\varphi_i = \left(\frac{t_i - T_0}{P_{\text{orb}}} \right) \bmod 1 \quad (2)$$

where t_i is the time of each data point, P_{orb} the orbital period, and T_0 the reference time (inferior conjunction). Both P_{orb} and T_0 have associated uncertainties, so the calculated orbital phase value will also have an uncertainty which grows with time elapsed since the ephemeris epoch:

$$u(\varphi) = \frac{1}{P_{\text{orb}}} \sqrt{u(T_0)^2 + N_i^2 u(P_{\text{orb}})^2} \quad (3)$$

where $u(A)$ is the uncertainty in quantity A , and $N_i = (T_0 - t_i)/P_{\text{orb}}$ is the number of orbital cycles that has elapsed between the reference epoch T_0 and the observation time t_i . For both events observed in Aql X-1, the phase is consistent with the range of orbital phases where dipping is most common for LMXBs (taking into account the uncertainty). We estimate the probability of such an agreement by chance as approximately 2.6%.

We calculated the equivalent exposure time for dips in the *RXTE* sample as the (fractional) number of orbital cycles for which

Table 1. Aql X-1 dip candidates and their associated properties

T_{cand} (MJD)	obsid	σ_{soft}	σ_{hard}	φ
53715.173(1)	91414-01-08-00	8.3	6.4	0.92 ± 0.06
55855.583(1)	96440-01-02-02	7.7	8.2	0.03 ± 0.09

the entire phase range of interest (0.7–1.0) would be covered. For Aql X-1, we calculate the total exposure in this phase range as 26.7 cycles. We then estimated the average likelihood of dips for Aql X-1 as 2 per 26.7 equivalent cycles covered, or an overall dip frequency of roughly $2/26.7 = 0.075 \text{ cycle}^{-1}$. By assuming that the number of dips detected is Poisson-distributed, we can more precisely estimate the likely range of the dip occurrence frequency of $0.10^{+0.07}_{-0.05} \text{ cycle}^{-1}$. In practise, the data covering each dip phase may be incomplete, interrupted by (satellite) orbital data gaps and scheduled observations of other sources. We may have missed additional dips in those data gaps, due to incomplete coverage of the dip phase. Thus, the dip occurrence frequency calculated above must be considered a lower limit to the actual dip frequency.

3.2 Spectral analysis of dip candidates in Aql X-1

Here we compare the X-ray spectrum measured by the PCA in the dip intervals, to the rest of each observation. For the observation on 2011 Oct 21 (ID 96440-01-02-02), only PCU #2 was operational, and we found the best fit to the observation-averaged spectrum with a model consisting of a Comptonisation continuum (compTT in XSPEC; Titarchuk 1994) also with a Gaussian component to model the Fe $K\alpha$ fluorescence line around 6.4 keV. The model included the effects of absorption by neutral material along the line-of-sight, with column density frozen at $n_H = 4 \times 10^{21} \text{ cm}^{-2}$ (Campana & Stella 2003). The assumed systematic error, following the recommendations of the instrument team, was 0.5%.

We subsequently divided up the observation into five separate dip segments (labeled 1, 2, 3a, 3b, and 4; Fig. 2), and extracted a spectrum for each of these segments, as well as a spectrum excluding all of the dip intervals, for comparison. Because the time resolution for Standard-2 data is 16 s, and the dip intervals identified did not correspond exactly to the start and end times of the 16-s bins, we extracted 64-channel spectra from Event-mode data, and calculated spectral responses and background appropriately. We then performed a joint fit of the non-dip and dip spectra, with a spectral model based on the best-fit model for the average, and experimented with freeing joint parameters between the spectra to determine the best way to model the variations during the dips.

We found that freeing the Comptonisation component normalisation alone, while leaving the n_H fixed at $4 \times 10^{21} \text{ cm}^{-2}$, did not give a satisfactory fit ($\chi^2_{\nu} = 13.97$ for 169 degrees-of-freedom). A similar result was obtained if the Gaussian normalisation was also thawed between the dips ($\chi^2_{\nu} = 13.71$). Conversely, a fit where the neutral column density n_H alone was free to vary between the dip and non-dip spectra, also resulted in a statistically unacceptable fit ($\chi^2_{\nu} = 2.89$).

Allowing both the Comptonisation component normalisation, and the n_H column density to vary between the dips (while leaving n_H frozen at $4 \times 10^{21} \text{ cm}^{-2}$ for the non-dip spectrum) gave a much better fit, with $\chi^2_{\nu} = 230.55/165 = 1.397$. The largest fitted column density was $(27.9 \pm 1.2) \times 10^{22} \text{ cm}^{-2}$ for interval 2, with the other dips exhibiting fitted column densities between $(6\text{--}19) \times 10^{22} \text{ cm}^{-2}$.

We found similar results for the single dip observed in the 2005 December observation. Here we extracted a single spectrum

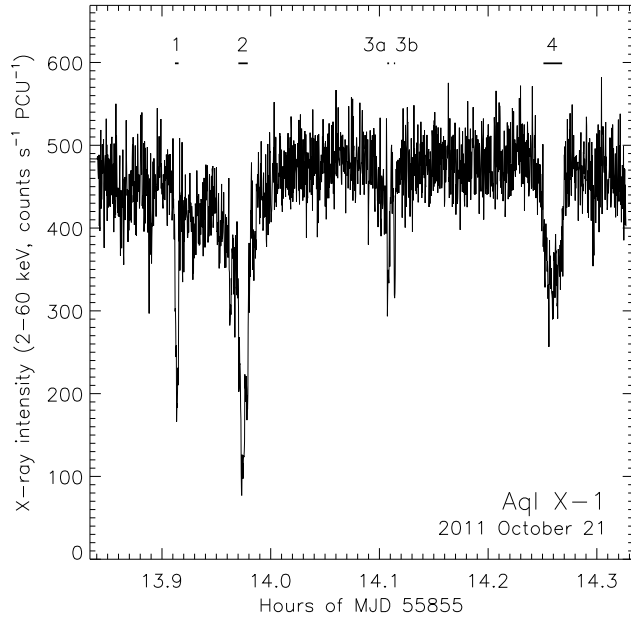


Figure 2. X-ray intensity of Aql X-1 during the RXTE observation on 2011 October 21 (obsid 96440-01-02-02). Shown is the 1-s binned lightcurve of the Standard-1 mode data, which includes photons in the energy range 2–60 keV. Note the multiple deep dip features, numbered 1, 2, 3a, 3b and 4; the thick black lines indicate the extent of spectral extraction for each dip. The lightcurve has been background subtracted and corrected to the solar system barycentre.

for the sole dipping episode (labeled as “Interval 1” in Table 2), with duration 32 s, and a comparison spectrum excluding this interval. As before, a *compTT* continuum component with a Gaussian simulating an Fe K α emission line provided the best overall fit, with the n_H value during the dip significantly in excess of the non-dip value, at $(14.0 \pm 0.5) \times 10^{22} \text{ cm}^{-2}$. However, the scattering electron temperature kT_e could not be constrained. This did not affect the overall quality of the fit, but did result in a disproportionately lower value of the *compTT* normalisation, because the integrated flux of this component also depends on the other spectral parameters via the scattering temperature and optical depth (note the absence of a prefactor for the K_{compTT} parameter for the 2005 December fits in Table 2). The combined fit of the dip and non-dip spectra achieved a χ^2 fit statistic of 133.2 for 101 degrees of freedom, indicating a statistically acceptable fit.

3.3 Search for dips from other LMXBs

We repeated the dip search for non-dipping sources² for which we had data in-hand as part of the MINBAR sample (Table 3). We prioritised the sources based on the total exposure accumulated with RXTE over the mission, and terminated our search when the estimated number of dip phases observed dropped below 1 (see §4.1). No plausible dip candidates were detected. Ideally such a search would also be extended to the non-bursting LMXBs, but analysis data for those sources were not available. Since the burster sample represents approximately half the known LMXB population (e.g.

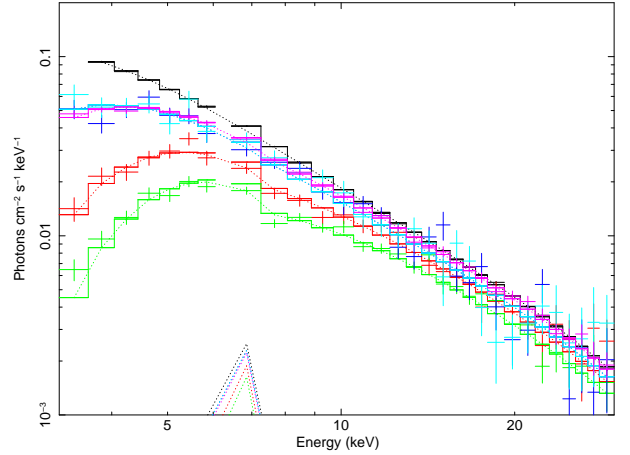


Figure 3. X-ray spectra of Aql X-1 during the dipping event of 2011 October 21. Shown are the PCU #2 spectra (*crosses*) and best-fit model curves (*solid histograms*) for each of the non-dip *black*, and dip spectra. Each of the dip intervals 1, 2, 3a, 3b and 4 are plotted with a different colour: red, green, blue, aqua, and magenta, respectively. Note the disproportionate reduction in the intensity below ≈ 6 keV for the dip spectra, most notable for the dip 2 interval (*green*).

Liu et al. 2007), we might expect at most one additional intermittent dipper to be detectable.

The best candidate for dips in sources other than Aql X-1 was in Cyg X-2, which exhibited in a few observations a pattern of intensity decreases, similar to that observed during dips. During some (but not all) of these intervals of lower intensity, the soft and hard colours were elevated, but not significantly. Spectral analysis of the best candidate dip interval, in observation 70016-01-01-00, exhibited no significant increase in the column density. Thus, we expect that the intensity variations may be due to other causes than dips.

As for Aql X-1, for those systems with measured orbital ephemerides, we summed the total exposure in the RXTE sample over the phase range in which dips are expected. 4U 1636–536 had the largest total exposure, with 682 total orbit equivalents. With no dips detected, we can calculate an upper limit on the dip rate, of $4.4 \times 10^{-3} \text{ cycle}^{-1}$ (95%). This is more than an order of magnitude lower than the estimated frequency for Aql X-1 (§3.1), indicating that we can rule out intermittent dipping behaviour conclusively in this system. Despite the smaller total exposure compared to 4U 1636–536, an even larger number of dip phases was observed for the ultracompact binary 4U 1820–303, due to the 11.46 min orbit. The total number of complete dip phases covered was 2186, leading to an upper limit on the dip rate of $1.4 \times 10^{-3} \text{ cycle}^{-1}$ (95%). This limit is difficult to reconcile with the claim of a dipping event by Cominsky et al. (1985).

4 DISCUSSION

The intermittent decrease in intensity observed during two outbursts of Aql X-1, within the orbital phase range in which dipping behaviour is seen in other LMXBs, and coupled with the evidence for elevated neutral column density, confirms these events as arising from the same physical cause as the regular dips seen in high-inclination LMXB systems.

These events are the first confirmed “intermittent” dips in a LMXB system, although not the first claimed. The candidate event reported from HEAO A-2 data of 4U 1820–303 (Cominsky et al.

² See <http://burst.sci.monash.edu/sources>

Table 2. Spectral characteristics of Aql X-1 data during the dipping episodes in 2005 December 11 and 2011 October 21.

Parameter	units	non-dip	1	Interval 2	3a & 3b	4
2005 December 11						
Time range	s from start	0–3420 excluding dips	1783–1815			
n_H	10^{22} cm^2	(0.4)	14.0 ± 0.5			
E_{Fe}	keV	(6.4)				
σ_{Fe}	keV	$1.09^{+0.06}_{-0.07}$				
K_{Fe}	$10^{-3} \text{ photons cm}^{-2} \text{ s}^{-1}$	5.0 ± 0.4				
T_0	keV	0.755 ± 0.009				
kT	keV	> 124				
τ		$(1.58^{+1.80}_{-0.04}) \times 10^{-2}$				
K_{compTT}	10^{-3}	$0.886^{+0.401}_{-0.007}$	$0.744^{+0.338}_{-0.011}$			
χ^2 (dof)		133.2(101)				
2011 October 21						
Time range	s from start	0–3420 excluding dips	1779–1791	1989–2020	2482–2488, 2504–2508	2999–3061
n_H	10^{22} cm^2	(0.4)	18.7 ± 1.2	27.9 ± 1.2	6.0 ± 0.8	8.0 ± 0.3
E_{Fe}	keV	6.60 ± 0.10				
σ_{Fe}	keV	(0.5)				
K_{Fe}	$10^{-3} \text{ photons cm}^{-2} \text{ s}^{-1}$	3.9 ± 0.6				
T_0	keV	0.894 ± 0.013				
kT	keV	$8.83^{+0.42}_{-0.36}$				
τ		3.13 ± 0.11				
K_{compTT}		0.101 ± 0.005	0.084 ± 0.005	0.073 ± 0.004	0.089 ± 0.005	0.098 ± 0.005
χ^2 (dof)		230.6 (179)				

Table 3. Low-mass X-ray binaries for which dip searches were carried out

Source name	R.A.	Dec.	P_{orb} (hr)	Tot. exp (ks)	Ref.
Aql X-1	19 11 16.05	+00 35 05.8	18.95	1850	Welsh et al. (2000)
4U 1636–536	16 40 55.50	–53 45 5.0	3.8	4270	Casares et al. (2006)
XTE J1701–462	14 00 58.50	–46 11 8.60		2730	
4U 0614+09	6 17 7.3	+09 8 13	0.50–0.83?	2680	Baglio et al. (2014); Madej et al. (2013)
Cyg X-2	21 44 41.2	+38 19 18.0	236.2	2230	Premachandra et al. (2016)
4U 1608–522	16 12 43.05	–52 25 23	12.89	2080	Wachter et al. (2002)
4U 1728–34	17 31 57.5	–33 50 5	0.18?	1680	Galloway et al. (2010)
4U 1820–303	18 23 40.5	–30 21 40.1	0.19	1500	Anderson et al. (1997)
4U 0513–40	05 14 6.6	–40 2 37	0.283	1490	Fiocchi et al. (2011)
SAX J1808.4–3658	18 08 27.5	–36 58 44.3	2.01365	1420	Chakrabarty & Morgan (1998)
4U 1705–44	17 8 54.5	–44 6 7.4		1240	
4U 1702–429	17 6 15.3	–43 02 8.7		1210	
XTE J1810–189	18 10 20.7	–19 04 11		1150	
GX 17+2	18 16 1.4	–14 02 11		1120	
4U 1735–444	17 38 58.3	–44 27 00	4.65	1003	Casares et al. (2006)
GS 1826–24	18 29 28.2	–23 47 29	2.088	958	Homer et al. (1998)
HETE J1900.1–2455	19 00 9.8	–24 54 4.3	1.38757	775	Kaaret et al. (2006)
2S 0918–549	09 20 27	–55 12 24.7		552	
4U 1722–30	17 27 33.2	–30 48 07		534	
GX 3+1	17 47 56	–26 33 49		518	
XTE J1710–281	17 10 12.3	–28 07 54	3.28	454	Jain & Paul (2011)
SAX J1748.9–2021	17 48 53.5	–20 22 02		375	
IGR J17511–3057	17 51 09	–30 57 40	3.4688	366	Riggio et al. (2011)
4U 1246–588	12 49 39.6	–59 05 13.3		199	
GRS 1741.9–2853	17 45 2.3	–28 54 49.9		42.3	

1985) helped to motivate our own search of 1500 ks of *RXTE* observations of this source, comprising 2186 total orbit equivalents of exposure in the 0.7–1.0 phase range. However, this search resulted in no plausible dip candidates.

Spectral analysis of the dipping events observed in Aql X-1 in-

dicates that both the neutral column density n_H and the continuum normalisation K_{compTT} vary significantly compared to the non-dip spectra. This behaviour is commonly found in (consistently) dipping systems (e.g. Smale et al. 1992; Díaz Trigo et al. 2006), and has been attributed to absorption by partially ionised material, pos-

sibly with abundances deviating significantly from solar, and/or partial covering of the (possibly extended) emission region.

While the complete sample of *RXTE* observations of Aql X-1 have covered other inferior conjunctions, no additional dipping behaviour has been observed. Based on the total exposure of the orbital phase in which dips are most often observed in other sources, we estimate the average frequency for dips in Aql X-1 as $0.10^{+0.07}_{-0.05} \text{ cycle}^{-1}$.

We also searched the accumulated *RXTE* data from 24 other systems for intermittent dipping activity, without success. For the system with the largest exposure of the dip phase range, 4U 1820–303, we place an upper limit on the dip frequency of $1.4 \times 10^{-3} \text{ cycle}^{-1}$ (95%).

The *RXTE* sample allows weak constraints to be placed on the duration of the dipping behaviour in Aql X-1. We inspected observations before and after each dip, selecting those data which fell in the usual dipping phase range of 0.7–1.0. We also searched for data covering the precise phase range of the deepest dipping features, since in other sources these features may persist for multiple orbital periods. For the 2005 December dip, we had partial coverage of the dipping phase range 3.9 d before and 1.4 d after. This corresponds to 5 cycles before and 2 after, with the data coverage of the range in each case totalling approximately 31%. We translate these figures to a $\approx 30\%$ chance of detecting dipping behaviour in each observation, had it been present; since no dips were detected, we can constrain the duration of the dipping behaviour to < 4.3 d (7 orbital cycles) at $0.3 \times 0.3 \approx 0.1$ confidence. Neither of these observations, however, included the precise orbital phase range in which the 2005 Dec dip was observed (Table 1). The closest coverage of that range was found 240 d before and after the dip observation.

Even poorer coverage was achieved for the 2011 October dip. The closest observation covering the 0.7–1.0 phase range before the dip was 388 d earlier; after, 6.9 d (9 cycles). The coverage of the dipping phase range for the latter observations was only 9%. The closest observations covering the precise phase range of the deepest dip observed in 2011 October were 684 d earlier, or 8.7 d (11 cycles) after. This latter observation likely provides the most stringent constraint on the duration of the dipping activity from the *RXTE* data.

4.1 The effect of system inclination

We consider three possible explanations for the apparent dipping behaviour in Aql X-1. First, that the system inclination is intermediate between the population of non-dippers and dippers, such that the normal activity of the disk occasionally allows material at the outer edge to cross the line of sight. According to this explanation, any system with an inclination within some range $\theta_1 < i < \theta_2$ would exhibit intermittent dipping behaviour, given enough observational data. To determine the probability distributions of the angles θ_1 , θ_2 , as well as the additional limit θ_3 above which a source will exhibit eclipses, we make the following assumptions: 1. the fraction of sources in each group is proportional to $(\cos \theta_i - \cos \theta_{i+1})$; 2. the number of sources detected in each category is Poisson-distributed about the expected value; 3. the expected number of intermittent dipping sources detected is lower by a factor of $(1 - 0.9^k)$, where k is the typical number of dip phase orbit equivalents observed for each source. This latter factor incorporates both the estimated frequency of dips for intermittent sources, as measured in Aql X-1, as well as the typical number of dip phases observed. Here we adopt the median *RXTE* exposure for all the burst sources of 55 ks, and the median orbital period, of 4.65 hr, to calculate $k \approx 1$.

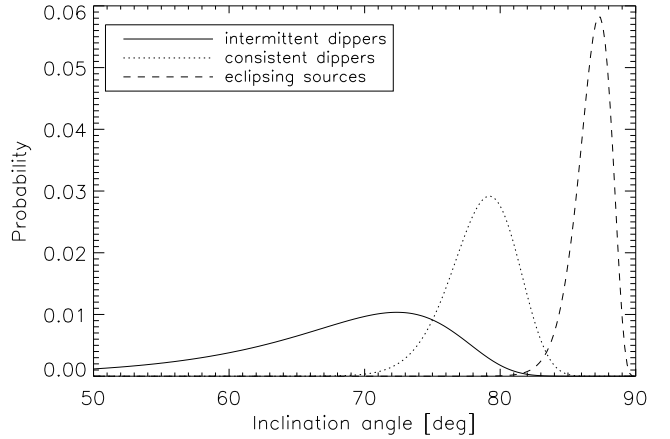


Figure 4. Inferred probability distributions for angle limits between non-dippers and intermittent dippers θ_1 (solid line); intermittent and consistent dippers θ_2 (dotted line); and dippers and eclipsing sources θ_3 (dashed line). The probability distributions are based on the fraction of dipping and eclipsing sources in the MINBAR sample of bursters. The overall normalisation scale is arbitrary, but consistent for each angle.

For each angle θ_i we then marginalise over the other two angles, adopting the observed population of intermittent dipping:consistently dipping:eclipsing sources, of 1:14:5 (from a total of 106) to obtain the probability distributions as plotted in Fig. 4. We find that the most probable range for each angle is $\theta_1 = 72^{+2}_{-14}$, $\theta_2 = 79.3^{+1.8}_{-3.2}$, and $\theta_3 = 87.2^{+0.7}_{-1.8}$ (68% confidence; central value given has the highest probability of the PDF). We note that the width of the distribution for θ_1 is quite sensitive to the value adopted for k . Our analysis suggests that the inclination for Aql X-1 is in the range $72\text{--}79^\circ$. Previous estimates of the inclination of Aql X-1 based on optical light curve modelling were confounded by the contribution of light from a nearby unrelated star (Chevalier et al. 1999; see also Cornelisse et al. 2007). The derived range from our analysis is broadly consistent with the estimate of Garcia et al. (1999) based on the photometric modulation during outburst, of $\approx 70^\circ$. Interestingly, the additional evidence for high inclination provided by the detection of dips, lends further support to the case for a massive ($\geq 2.7 M_\odot$) neutron star (Cornelisse et al. 2007).

Since the estimated inclination range for the intermittent dippers is so wide, there are likely ≈ 15 other intermittent dippers in the burster sample, and perhaps the same number in the non-burster LMXB population. That dips have not been detected from any of these ≈ 30 other systems is a consequence of the low dipping frequency, as well as the paucity of data covering the preferred dip orbital phase.

4.2 Alternative explanations for the intermittent dips

A second possibility for the presence of intermittent dips in Aql X-1 is that the accretion disk in this system is subject to precession, such that the normal vector to the disk plane rotates around the orbital angular momentum axis, bringing the outer edge of the disk into the line-of-sight periodically. Precession in LMXBs is perhaps best known in the pulsar Her X-1 (e.g. Ogilvie & Dubus 2001), where a 35-d “superorbital” cycle has the disk periodically obscuring the pulsar at its centre. Precession has been suggested to explain quasi-periodic variability of persistent LMXBs (e.g. 4U 1728–34, Galloway et al. 2003), but the relatively subtle effects would likely

be indistinguishable from the much higher amplitude variability in transients. While our results allow candidate precession periods to be calculated, these are not constrained due to the limited number of events (2). Furthermore, it is not clear if a precession signal would persist over multiple outburst-quiescence cycles.

Third, the serendipitous observation of dips may be related to changes in the disk structure, perhaps resulting from a change in the disk geometry (signalled by a spectral state transition; e.g. Done et al. 2007) around the time of the dips. In the *RXTE* observations subsequent to the 2011 dip, from October 24 onwards, the overall intensity was significantly higher, with soft colour remaining between 1.2–1.3, but the hard colour decreasing to between 0.32–0.4. This increase in intensity, coupled with spectral softening, likely indicates a transition from the “island” (hard) spectral state to the “banana” (soft) state some time between October 21 and 24. However, no such transition was observed around the time of the 2005 dip, nor at anytime during that outburst, which was much weaker than that in 2011.

5 CONCLUSIONS

We report the detection by *RXTE* of a pair of events in Aql X-1 with properties consistent with the dips found in a subset of low-mass X-ray binaries. These events are the first such “intermittent” dips confirmed for a LMXB; given the accumulated exposure on this source, the estimated rate of such events is $0.10^{+0.07}_{-0.05} \text{ cycle}^{-1}$. The spectral analysis of the dip segments shows that the inferred neutral column density n_H is elevated typically by an order of magnitude, and up to almost two orders of magnitude, compared to the non-dipping value. Assuming that the dips arise in Aql X-1 by virtue of a higher-than-average inclination, the implied range is $72\text{--}79^\circ$; this is in excess of most other estimates for the source. Given the difficulty of detecting such events in other systems, it is possible that an additional 15 systems may be undetected intermittent dippers. Of the possible explanations of the intermittent dipping behaviour, the high inclination seems the most plausible. We also report on a search of 24 additional systems for dips, which was unsuccessful. For the system with the largest exposure, 4U 1636–536, we derive an upper limit on the dip rate of $4.4 \times 10^{-3} \text{ cycle}^{-1}$ (95%).

ACKNOWLEDGEMENTS

DKG acknowledges the support of an Australian Research Council Future Fellowship (project FT0991598). This paper utilizes preliminary analysis results from the Multi-INstrument Burst ARchive (MINBAR), which is supported under the Australian Academy of Science’s Scientific Visits to Europe program, and the Australian Research Council’s Discovery Projects funding scheme. This research has made use of data and software provided by the High Energy Astrophysics Science Archive Research Center (HEASARC), which is a service of the Astrophysics Science Division at NASA/GSFC and the High Energy Astrophysics Division of the Smithsonian Astrophysical Observatory.

REFERENCES

Anderson, S. F., Margon, B., Deutsch, E. W., Downes, R. A., & Allen, R. G. 1997, *ApJ*, 482, L69
 Baglio, M. C., Mainetti, D., D’Avanzo, P., et al. 2014, *A&A*, 572, A99
 Campana, S., Coti Zelati, F., & D’Avanzo, P. 2013, *MNRAS*, 432, 1695

Campana, S., & Stella, L. 2003, *ApJ*, 597, 474
 Casares, J., Cornelisse, R., Steeghs, D., et al. 2006, *MNRAS*, 373, 1235
 Chakrabarty, D., & Morgan, E. H. 1998, *Nature*, 394, 346
 Chevalier, C., Ilovaisky, S. A., Leisy, P., & Patat, F. 1999, *A&A*, 347, L51
 Cominsky, L., Simmons, J., & Bowyer, S. 1985, *ApJ*, 298, 581
 Cominsky, L. R., & Wood, K. S. 1984, *ApJ*, 283, 765
 Cornelisse, R., Casares, J., Steeghs, D., et al. 2007, *MNRAS*, 375, 1463
 Díaz Trigo, M., Parmar, A. N., Boirin, L., Méndez, M., & Kaastra, J. S. 2006, *A&A*, 445, 179
 Done, C., Gierliński, M., & Kubota, A. 2007, *A&ARv*, 15, 1
 Fiocchi, M., Bazzano, A., Natalucci, L., Landi, R., & Ubertini, P. 2011, *MNRAS*, 414, L41
 Galloway, D. K. 2012, *The Astronomer’s Telegram*, 4014
 Galloway, D. K., Muno, M. P., Hartman, J. M., Psaltis, D., & Chakrabarty, D. 2008, *ApJS*, 179, 360
 Galloway, D. K., Psaltis, D., Chakrabarty, D., & Muno, M. P. 2003, *ApJ*, 590, 999
 Galloway, D. K., Yao, Y., Marshall, H., Misanovic, Z., & Weinberg, N. 2010, *ApJ*, 724, 417
 Garcia, M. R., Callanan, P. J., McCarthy, J., Eriksen, K., & Hjellming, R. M. 1999, *ApJ*, 518, 422
 Güngör, C., Güver, T., & Ekşi, K. Y. 2014, *MNRAS*, 439, 2717
 Homer, L., Charles, P. A., & O’Donoghue, D. 1998, *MNRAS*, 298, 497
 Iaria, R., Di Salvo, T., Burderi, L., et al. 2014, *A&A*, 561, A99
 Jahoda, K., Swank, J. H., Giles, A. B., et al. 1996, *Proc. SPIE*, 2808, 59
 Jain, C., & Paul, B. 2011, *MNRAS*, 413, 2
 Kaaret, P., Morgan, E. H., Vanderspek, R., & Tomsick, J. A. 2006, *ApJ*, 638, 963
 Liu, Q. Z., van Paradijs, J., & van den Heuvel, E. P. J. 2007, *A&A*, 469, 807
 Madej, O. K., Jonker, P. G., Groot, P. J., et al. 2013, *MNRAS*, 429, 2986
 Morgan, E. H., Remillard, R. A., & Garcia, M. R. 1988, *ApJ*, 324, 851
 Motch, C., Pedersen, H., Courvoisier, T. J.-L., Beuermann, K., & Pakull, M. W. 1987, *ApJ*, 313, 792
 Ogilvie, G. I., & Dubus, G. 2001, *MNRAS*, 320, 485
 Parmar, A. N., White, N. E., Giommi, P., & Gottwald, M. 1986, *ApJ*, 308, 199
 Premachandra, S. S., Galloway, D. K., Casares, J., Steeghs, D. T., & Marsh, T. R. 2016, *ApJ*, 823, 106
 Riggio, A., Papitto, A., Burderi, L., et al. 2011, *A&A*, 526, A95
 Rodriguez, J., & Shaw, S. E. 2005, *The Astronomer’s Telegram*, 660
 Smale, A. P., Mukai, K., Williams, O. R., Jones, M. H., & Corbet, R. H. D. 1992, *ApJ*, 400, 330
 Titarchuk, L. 1994, *ApJ*, 434, 570
 Wachter, S., Hoard, D. W., Bailyn, C. D., Corbel, S., & Kaaret, P. 2002, *ApJ*, 568, 901
 Walter, F. M., Mason, K. O., Clarke, J. T., et al. 1982, *ApJ*, 253, L67
 Waterhouse, A. C., Degenaar, N., Wijnands, R., et al. 2016, *MNRAS*, 456, 4001
 Welsh, W. F., Robinson, E. L., & Young, P. 2000, *AJ*, 120, 943
 White, N. E., & Mason, K. O. 1985, *Space Sci. Rev.*, 40, 167
 White, N. E., & Swank, J. H. 1982, *ApJ*, 253, L61
 Yamaoka, K., Krimm, H. A., Tomsick, J. A., et al. 2011, *The Astronomer’s Telegram*, 3686

This paper has been typeset from a \LaTeX file prepared by the author.